

ChemComm

Accepted Manuscript



This is an *Accepted Manuscript*, which has been through the Royal Society of Chemistry peer review process and has been accepted for publication.

Accepted Manuscripts are published online shortly after acceptance, before technical editing, formatting and proof reading. Using this free service, authors can make their results available to the community, in citable form, before we publish the edited article. We will replace this *Accepted Manuscript* with the edited and formatted *Advance Article* as soon as it is available.

You can find more information about *Accepted Manuscripts* in the [Information for Authors](#).

Please note that technical editing may introduce minor changes to the text and/or graphics, which may alter content. The journal's standard [Terms & Conditions](#) and the [Ethical guidelines](#) still apply. In no event shall the Royal Society of Chemistry be held responsible for any errors or omissions in this *Accepted Manuscript* or any consequences arising from the use of any information it contains.

COMMUNICATION

Detecting miRNA by producing RNA: a Sensitive Assay that combines Rolling-Circle DNA polymerization and Rolling Circle Transcription

Cite this: DOI: 10.1039/x0xx00000x

Received 00th January 2012,
Accepted 00th January 2012

Xuemei Li,^a Fuwei Zheng^b and Rui Ren^{a*}

DOI: 10.1039/x0xx00000x

www.rsc.org/

Target miRNA was detected by producing RNA: Rolling Circle Polymerization (RCP) and Rolling Circle Transcription (RCT) were interlinked to provide dual amplification, producing multiplied malachite green (MG) aptamers; and signal was generated by the SERS (surface-enhanced Raman scattering) quantification of the MG molecules that was bound to the transcripts.¹

MicroRNAs (miRNA for short) refer to a category of non-coding endogenous RNAs, whose name came from their micro size (usually 20~25 nucleotides). The fundamental functions of miRNAs are RNA silencing and the post-translational regulation of gene expression. Recently, detection of miRNA attracted much attention because of their roles in cancer and other diseases: on one hand, dysregulation and aberrant expression of miRNAs were associated with certain diseases;¹ on the other hand, for metastatic cancer of unknown primary origin, the occurrence of the miRNAs can be used to identify the tissue origin of the cancer.² Furthermore, miRNA detection was challenged by the fact that they often occurred in organism in families with quite similar length and sequence (typically, let7 family), but different functions; thus it was of vital importance for any miRNA assay to distinguish among such miRNAs. To meet this challenge, efforts had been focused on developing specific and sensitivity assays for miRNA.³

Rolling Circle Amplification (RCA) is a well-known biochemical reaction in which a long DNA strand with tandem periodic segments was produced through the DNA polymerization

using a closed single-stranded DNA circle as the template.⁴ It was widely used in the bioassays for signal amplification,⁵ where it is also often referred to as RCA (Rolling Circle Amplification). Rolling Circle Transcription (RCT) is a biochemical reaction that generates long RNA chain with tandem periodic segments through RNA polymerization using a double-stranded DNA circle as the template.⁶ Despite being an obvious analogue to the RCP, RCT was not often used in bioanalysis, especially, rarely used in the assays based on nucleic acid molecular machines⁸ (or say, artificially bottom-up engineered automatic protocols). Instead, RCT was often seen used in top-down analysis⁹ or the construction of RNA nanostructures.¹⁰

Malachite Green (MG) is an organic dye which was reported to have an RNA aptamer that binds with it specifically. MG found its usage in bioanalysis for such a binding would indicate the production or the existence of RNA.¹¹ As a typical example, this feature was coupled with RCT to build a sensitive assay,¹² as one of the rare examples of the usage of RCT in bioanalysis - it was

SERS, or Surface-Enhanced Raman Scattering, was widely used in bioanalysis in recent years since it is capable of characterization and quantification at the same time: on one hand, Raman scattering spectra were specific to the target molecules; on the other hand, after being enhanced 10^7 ~ 10^{14} times by roughened metal surface or nanopores, the Raman scattering could be used as a sensitively quantitative signal generation.^{13, 14}

So far, no study that involves RCP and RCT in the same amplification system has been reported. In this study, these two components were interlinked to build a novel amplification protocol, which was coupled with SERS to build a selective and sensitive assay for miRNA.

The principle of the study involved a reaction system and a circular probe. In the reaction system, RCP and RCT were included for amplification; and, an interlinking stage to convey the amplification of RCP to RCT; also a tailored recognition mechanism for recognizing the target miRNA, and MG-aptamer binding process to produce the signal were also included.

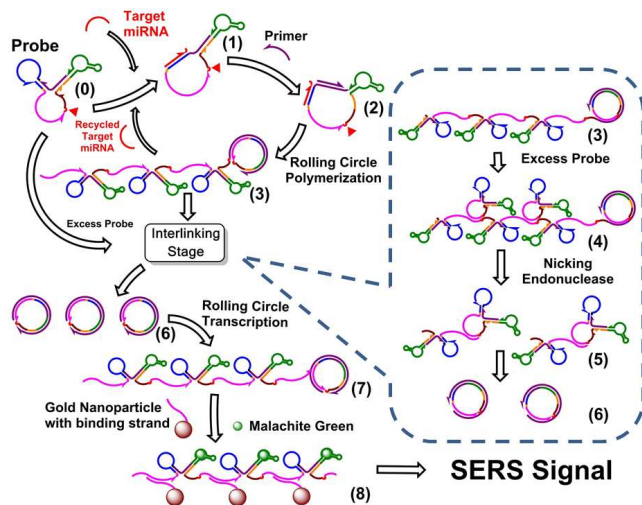
The circular probe is an artificially designed single-stranded circular DNA structure on which the reaction system was based. The details of the probe can be found in ESI. On the probe the following functional segments were placed: "Trigger site" (color coded blue), which specifically recognized the target

^a Shandong Province Key Laboratory of Detection Technology for Tumor Markers, College of Chemistry and Chemical Engineering, Linyi University, Linyi 276005, P. R. China,

^b Key Laboratory of Sensor Analysis of Tumour Marker, Ministry of Education, College of Chemistry and Molecular Engineering, Qingdao University of Science and Technology, Qingdao 266042, P. R. China

† Electronic Supplementary Information (ESI) available: [details of any supplementary information available should be included here]. See DOI: 10.1039/c000000x/

miRNA; “Primer switch” (color coded violet), a dynamic segment that is complementary to the primer, which is sufficiently “blocked” at the initial state; this switch was designed to be coupled to the “recognizing trigger”: opening of the latter would cause the opening of the former. “MG aptamer template” (color coded green), the DNA segment with complementary sequence to the RNA aptamer of MG; the “nicking switch” (color coded red), half of the double-stranded nicking site of the nicking endonuclease; it can bind with its complementary strand to form a functional double-stranded nicking site; and “Promoter switch” (color coded magenta), half of the functional double-stranded T7 promoter. In practice, the probe was built by ligating two strands (see ESI for details) so that the design can be generalized by altering one of them.



Scheme 1 The Principle of the detection system. Details can be found in Scheme S1 to S4 in ESI.

The principle of the assay was shown in Scheme 1 and Scheme S2 to S4 in ESI. The initial state of the detection reaction system consisted of intact probe (0) and primer of high concentration. When initialized by the target miRNA, the reaction system would finally turn the initial state into the signal compound, i.e. the RCT product combined with malachite green and the enhancing gold nanoparticle.

The triggering stage served as the starting of the whole reaction system. This stage started with the recognition of the target miRNA by the circular probe. The target miRNA hybridized with the trigger site in the probe (0), activating switch (1). Due to the coupling of the “trigger site” and the “primer switch”, the latter switch is also opened, leading to the binding of the primer, and thus the “initialized complex” (2) was formed, getting ready for the RCP stage.

In this stage, the miRNA was recognized solely through hybridization, which is well known to be sequence-specific. Thus the triggering stage, and also the whole detection, was also sequence-specific to the target miRNA.

Rolling Circle Polymerization occurred on the basis of the “initialized complex” (2) with the aid of DNA polymerization and dNTPs, posing primary amplification; as a result, a long DNA strand with tandem periodic segments (“RCP product”, (3)) was produced, in which each segment bearing the sequence complementary to that of the circular probe.

On the other hand, in the “initialized complex”, the miRNA was still attached on the probe without triggering any polymerization due

to the design of this site (see ESI for details). In the RCP, due to the strand-displacing characteristic of DNA polymerization, the target was expected to be replaced by the newly-generated product strand and released into the solution, and thus being available again for another triggering. Through this process, the target miRNA was expected to be utilized in a cycling mode.

In the RCP stage, amplification was provided in two ways. First, the multiplied segments in the RCP products combined with the excess probe molecules to produce multiplied RCT template (relative to the “initialized complex”). Second, the cycling of miRNA increased the turnover of the RCP reaction, posing further amplification.

After RCP, the reaction system underwent a process that interlinked RCP and RCT (“interlinking stage”). This stage made use of the RCP products and the excess circular probe to prepare for the RCT stage. As the target miRNA was of tiny quantity (relative to the probe), the probe were excess in the reaction mixture, which would hybridize with the RCP products (4), and double-stranded nicking sites would be formed, where the RCP product could be nicked, producing fragments with one or several repetitive units (5). These fragments would then turn into double-stranded circular complexes; these complexes bore double-stranded functional promoters, and thus the RCT template (6) was ready.

And then Rolling Circle Transcription occurred on the RCT template, posing a secondary amplification over the primary amplification, and resulting in the RCT product that would lead to the signal. The RCT template (6) was a hybridization complex of the circular probe and its complementary strand (nicking products of the RCP product), in which the promoter segment was double-stranded. Rolling circle transcription occurred from this site, producing a long RNA strand with tandem periodic segments, each segment bearing a sequence of the MG aptamer (7). Although the nicked RCP product was not a closed circle, RCT could still occur since it was actually based on the anti-sense strand in the template, i.e. the circular probe.

Signal and detection – In this section, SERS signal was generated from the RCT products. MG was added and was caught by the MG aptamer sequences, and gold nanoparticles were attached on the RCT products for signal enhancement (8). After centrifugation and washing (see ESI for details), The Raman scattering signals were recorded on a Renishaw inVia Raman microscopy.

Despite of the numerous reactions and processes described above, the first three stages can be operated in one-pot mode. These reactions work automatically like a molecular machine - once being initiated by the target, they would occur successively and automatically all through the stages, until the RCT product was generated. This provides convenience and simplicity to the operation of the assay.

It can be experimentally verified that reaction system worked as described above. Non-denaturing polyacrylamide gel electrophoresis (PAGE) was carried out for the DNA reaction part, and TIRF imaging was used to verify the generation of the transcripts and its binding with MG molecule. The results were in accord with the aforementioned protocols (See Section 4 “PAGE characterization of the network” in ESI for details).

The optimal reaction conditions for the assay was determined to be reaction time of 3 h, DNA polymerase of $0.60 \text{ IU } \mu\text{L}^{-1}$, Nb.BbvCI (nicking endonuclease) of $0.40 \text{ IU } \mu\text{L}^{-1}$ and T7 RNA polymerase of $2.0 \text{ IU } \mu\text{L}^{-1}$ (see section 5 “Optimization of reaction conditions” and Figure S5 in ESI for details). Under the optimal conditions, the calibration curve was produced by plotting the normalized ΔI , the SERS response at 1614 cm^{-1} shift (after subtraction of the blank response) against the concentration of the target miRNA (C_{Target}). A linear regression relationship was observed between the SERS response and the logarithm of the target miRNA concentration

across a linear range from 10^{-16} M to 10^{-13} M. In this range, the regression equation was $\Delta I = 3.07 \lg c_{\text{Target}} + 49.83$, and the limit of the detection (LOD) was determined to be 6.63×10^{-17} M, according to the 3σ rule.

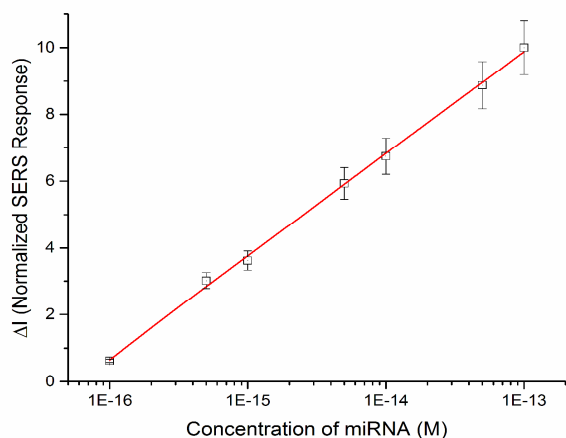


Fig. 1. Calibration Curve of the assay for miRNA. ΔI was normalized so that the response from the complete reaction system was 10.0 at the target miRNA concentration of 1.0×10^{-13} M.

To explore the role of the different parts in the reaction system, comparative amplification experiments were carried out in different modes. As the amplification of RCP itself had been illustrated in the previous study,⁸ this study would focus on two issues: how the extra amplification was superposed by RCP on the RCT, and, especially, what role did the interlinking stage play in the dual amplification system. Thus, the SERS responses of the following modes were investigated. The three modes were tested across a concentration gradient.

- The complete reaction system was carried out;
- “RCT only” mode: Only the RCT and signaling processes were carried out, using a prepared strand of known concentration to mimic the product of RCP and nicking;
- “Without nicking” mode: Triggering, RCP, RCT and signaling processes are carried out, while the nicking step was omitted by leaving out the nicking endonuclease from the reaction system;
- “No amplification” mode: as a basepoint for the comparison of amplification, the SERS responses of MG and its aptamer of known concentrations were measured, i.e. in the case no amplification was applied.

The comparison results were shown in Fig. 2, while the SERS responses can be found in Fig. S6 and S7 in ESI. Comparison of mode b) and mode d) indicated that RCT stage provide amplification of 10^3 to 10^4 times. Comparison of mode a) and mode b) indicated that extra amplification has been superposed on that of RCT by the RCP and the interlinking stage: to reach the same SERS response, the target miRNA concentration at 10^{-13} M grade was required in mode a), while 10^{-10} M was required in mode b), thus at this response level, the RCP and the interlinking steps superposed the amplification of about 10^2 to 10^3 times. Comparison of mode a) and mode d) show that the total reaction system provided amplification of about 10^6 times in all.

Comparison of mode b) and mode c) brought about another finding - the role of the interlinking stage in the whole detection system was to convey the amplification of the RCP stage to the downstream RCT stage. Mode c), although containing two built-in amplification steps (RCP and RCT), does not provide as much

amplification as in the mode a); Furthermore, the responses in the mode c) across the concentration gradient were even less than those in the mode b) at certain miRNA concentrations. This indicated that without the interlinking stage (the difference between mode c) and mode a)), the amplification of RCP did not contribute to the final response, or say, cannot be conveyed to the RCT stage. This result was in accordance with the assay protocol as designed: nicking step was crucial for the formation of the RCT template. Without nicking, the RCP products, being a long continuous strand, would not fully hybridize with the excess circular template; especially, the double-stranded promoter segment, which was essential for the starting of any transcription, would not be ideally formed, resulting in a situation that although RCP product was generated, the RCT was not sufficiently initiated and cannot provide as much amplification as in mode a). Thus, the role of the interlinking stage as described above can be verified from both mechanism and experimental aspects.

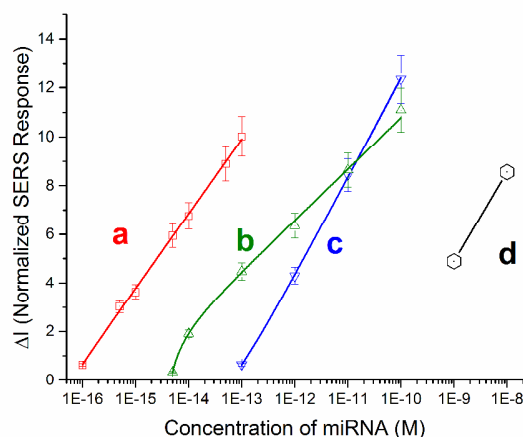


Fig. 2. Comparison of the performance of the complete reaction system with two contrast modes. a) Calibration curve of the whole system; b) calibration curve of “RCT only” mode; c) calibration curve of “without nicking” mode; d) the basepoint for comparison: SERS responses when no amplification were applied. ΔI was normalized so that the response from the complete reaction system was 10.0 at the target miRNA concentration of 1.0×10^{-13} M.

Given the well-established fact that the complex of MG and its RNA aptamer produced enhanced fluorescence, one might wonder why SERS was chosen for the signal in this study. Here a test was performed regarding this question: the signal stage was altered, namely, the attaching of the gold nanoparticle was omitted, and the fluorescence signal instead of SERS was recorded. The results (see Section S7 in ESI) indicated that SERS was much superior to fluorescence in sensitivity. Thus SERS was more preferred.

The sequence-specific triggering stage provided the reported assay with selectivity. The precursor of the target (pre-hsa-let-7a), three mismatched miRNAs from let-7 family, and the negative control (miRNA with same length but totally irrelevant sequence) were used to assess whether there was cross interference. Even at concentrations of the mismatched miRNAs and the negative control as high as 1.0×10^{-10} M, or the precursor at the concentration of 1.0×10^{-11} M, signals were distinguishable from the signal of 1.0×10^{-13} M target (Fig. S11 in ESI). Excellent selectivity was thus confirmed regarding the single-stranded miRNAs.

Performance in the detection of miRNA from biological real sample was also examined. First it was examined whether this assay could be interfered when being applied in biological matrix, namely, human serum (ESI). Then, this assay was further tested by detecting miRNA from HeLa cells. Total RNA was extracted from different

contents of HeLa cells and used as the analyte to be examined by the reported assay. The SERS responses (Fig. 3), after subtraction of the blank and normalization, were found to be in the linear relation with the logarithm of the cell contents in the range from 10^3 to 10^6 cells mL^{-1} , with the regression equation to be $\Delta I = 2.00 \lg c_{\text{Cell}} - 4.46$. The slope is somewhat lower than in the regression equation from the standard miRNA target, possibly resulted from the interference from other RNA species from the cells.

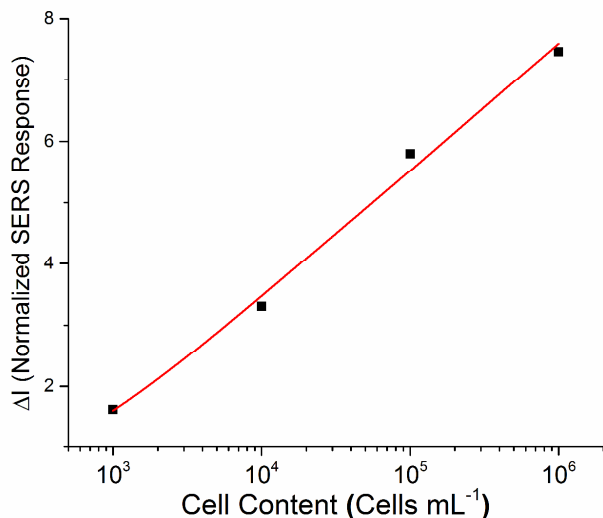


Figure 3. Calibration Curve of the assay for HeLa cells. ΔI was normalized so that the response from the complete reaction system was 10.0 at the target miRNA concentration of 1.0×10^{-13} M.

In conclusion, in this study, a sensitive and selective assay for miRNA was developed. Based on a specially-designed circular probe, the reaction system in this assay started with a tailored triggering strand for target recognition, featured the combination of Rolling Circle Polymerization (RCP) and Rolling Circle Transcription (RCT) that provided dual signal amplification, and generated the Surface-Enhanced Raman Scattering (SERS) signal from the malachite green bound on its aptamer. Specially, an interlinking stage was designed for the combination of RCP and RCT. Due to the design, most parts in the reaction system of the assay were automatic, thus the assay, except for the signal-producing stage, can be operated in one-pot mode. This assay can detect miRNA with high sensitivity, with detection limit well below 10^{-16} M, comparable or superior to the miRNA assays reported recently (Table S3 in ESI). It was testified that the interlinking stage was crucial in this enhancement of sensitivity, since it conveyed the amplification of RCP stage to the downstream RCT stages. The assay was also testified with good specificity due to the trigger stage was sequence-specific to the target miRNA. It was also resistant to the interference in the analyte matrix to certain extent, through the fact that it was capable to detect miRNA in biological matrix (serum for example) or real samples (RNA extracts from cells).

This work was supported by the National Natural Science Foundation of China (No. 21205066), the National Basic Research Program of China (No. 2010CB732404) and the Science and Technology Plan Projects of the Colleges of Shandong Province (J12LD14).

Notes and references

1 S. Volinia, G. A. Calin, C.-G. Liu et al., *Proc. Natl. Acad. Sci. USA.*, 2006, **103**, 2257

- 2 a) J. Lu, G. Getz, E. A. Miska et al., *Nature*, 2005, **435**, 834; b) N. Rosenfeld, R. Aharonov, E. Meiri et al., *Nat. Biotechnol.*, 2008, **26**, 462.
- 3 a) Y. Cheng, X. Zhang, Z. Li et al., *Angew. Chem. Intl. Ed.*, 2009, **48**, 3268; b) H. Jia, Z. Li, C. Liu et al. *Angew. Chem. Intl. Ed.*, 2010, **49**, 5498; c) S. Neubacher and C. Arenz, *ChemBioChem*, 2009, **10**, 1289; d) H.-M. Chan, L.-S. Chan, R. N.-S. Wong, *Anal. Chem.*, 2010, **82**, 6911; e) S. C. Chapin and P. S. Doyle, *Anal. Chem.*, 2011, **83**, 7179; f) L. Yang, C. Liu, W. Ren et al., *Appl. Mater. Interfaces*, 2012, **4**, 6450; g) F. Degliangeli, P. Kshirsagar, V. Brunetti, *J. Am. Chem. Soc.*, 2014, **136**, 2264; h) R. Deng, L. Tang, Q. Tian et al., *Angew. Chem. Intl. Ed.*, 2014, **53**, 2389
- 4 P. M. Lizardi, X. H. Huang, Z. R. Zhu et al., *Nat. Genet.*, 1998, **19**, 225;
- 5 a) E. J. Cho, L. T. Yang, M. Levy et al., *J. Am. Chem. Soc.*, 2005, **127**, 2022; b) Y. Cheng, X. Zhang, Z. Li et al., *Angew. Chem., Intl. Ed.*, 2009, **48**, 3268; c) T. Murakami, J. Sumaoka and M. Komiyama, *Nucleic Acids Res.*, 2009, **37**, e19; d) N. Li, C. Jablonowski, H. Jin and W. Zhong, *Anal. Chem.*, 2009, **81**, 4906; e) Y. Zhou, Q. Huang, J. Gao et al., *Nucleic Acids Res.*, 2010, **38**, e156; f) W. Xu, X. Xie, D. Li et al., *Small*, 2012, **8**, 1846; g) E. M. Harcourt and E. T. Kool, *Nucleic Acids Res.*, 2012, **40**, e65; h) Y. Long, X. Zhou and D. Xing, *Biosens. Bioelectron.*, 2013, **46**, 102.
- 6 a) J. M. Buzayan, W. L. Gerlach, G. Bruening, *Nature*, 1986, **323**, 349; b) S. L. Daubendiek and E. T. Kool, *Nat. Biotech.*, 1997, **15**, 273; c) A. M. Diegelman and E. T. Kool, *Nucleic Acid Res.*, 1998, **26**, 3235; d) M. Frieden, E. Pedroso and E. T. Kool, *Angew. Chem. Intl. Ed.*, 1999, **38**, 3654; e) D. Haussecker, D. Cao, Y. Huang, et al., *Nat. Struct. Mol. Biol.*, 2008, **15**, 714
- 7 A. Kristoffersson, *Master Thesis of Uppsala University*, 2010
- 8 K. Furukawa, H. Abe, N. Abe et al., *Bioorg. Med. Chem. Lett.*, 2008, **18**, 4562
- 9 Y. Dang and B. R. Green, *J. Biol. Chem.*, 2010, **8**, 5196
- 10 A) P. Guo, *Mol. Ther.–Nucleic Acids*, 2012, **1**, e36; b) J. B. Lee, J. Hong, D. K. Bonner et al., *Nat. Mater.*, 2012, **11**, 316; c) D. Han, Y. Park and H. Kim., *Nat. Commun.*, 2014, **5**, 4367; c) K. E. Shopsowitz, Y. H. Roh, Z. J. Deng, *Small*, 2014, **10**, 1623; d) H.-N. Zheng, Y.-Z. Ma and S.-J. Xiao, *Chem. Commun.*, 2014, **50**, 2100; e) D. Han, Y. Park and H. Nam., *Chem. Commun.*, 2014, **50**, 11665; f) F. J. Eber, S. Eiben, H. Jeske et al., *Nanoscale*, 2015, **7**, 344
- 11 A) D. Grate and C. Wilson, *Proc. Natl. Acad. Sci. USA.*, 1999, **96**, 6131; b) M. N. Stojanovic and D. M. Kolpashchikov, *J. Am. Chem. Soc.*, 2004, **126**, 9266; c) J. R. Babendure, S. R. Adams and R. Y. Tsieng, *J. Am. Chem. Soc.*, 2003, **125**, 14716
- 12 a) A. C. Bhasikuttan, J. Mohanty and H. Pal, *Angew. Chem. Intl. Ed.*, 2007, **119**, 9465; b) S. L. Stead, H. Ashwin and B. H. Johnston, *Anal. Chem.*, 2010, **82**, 2652; c) Y. Wu, S. Zhang and L. Xu, *Chem. Commun.*, 2011, **46**, 6027; d) K. A. Afonin, E. Bindewald, A. J. Yaghoobian et al., *Nat. Nanotech.*, 2010, **5**, 676
- 13 a) S. Lai, J. Wang, L. Luo et al., *Anal. Chem.*, 2004, **76**, 1832; b) G. Wang and R. J. Lipert, *Anal. Chem.*, 2011, **83**, 2554; c) M. Li, J. Zhang, S. Suri et al., *Anal. Chem.*, 2012, **84**, 2837.
- 14 a) Y. Li, C. Lei, Y. Zeng et al., *Chem. Commun.*, 2012, **48**, 10892; b) S. Ye, Y. Yang, J. Xiao et al., *Chem. Commun.*, 2012, **48**, 8538; c) S. Ye, Y. Guo, J. Xiao, *Chem. Commun.*, 2013, **49**, 3643; d) Y. Li, X. Qi, C. Lei et al., *Chem. Commun.*, 2014, **50**, 9907; e) Z. Zhang, Y. Wang, F. Zheng et al., *Chem. Commun.*, 2015, **51**, 907